25 November 1999

A study of the $\eta\eta'$ and $\eta'\eta'$ channels produced in central pp interactions at 450 GeV/c

The WA102 Collaboration

D. Barberis[4], F.G. Binon[6], F.E. Close[3,4], K.M. Danielsen[11], S.V. Donskov[5], B.C. Earl[3], D. Evans[3], B.R. French[4], T. Hino[12], S. Inaba[8], A. Jacholkowski[4], T. Jacobsen[11], G.V. Khaustov[5], J.B. Kinson[3], A. Kirk[3], A.A. Kondashov[5], A.A. Lednev[5], V. Lenti[4], I. Minashvili[7], J.P. Peigneux[1], V. Romanovsky[7], N. Russakovich[7], A. Semenov[7], P.M. Shagin[5], H. Shimizu[10], A.V. Singovsky[1,5], A. Sobol[5], M. Stassinaki[2], J.P. Stroot[6], K. Takamatsu[9], T. Tsuru[8], O. Villalobos Baillie[3], M.F. Votruba[3], Y. Yasu[8].

Abstract

The reactions $pp \to p_f(X^0)p_s$, where X^0 is observed decaying to $\eta\eta'$ and $\eta'\eta'$, have been studied at 450 GeV/c. This is the first time that these channels have been observed in central production and only the second time that the $\eta'\eta'$ channel has been observed in any production mechanism. In the $\eta\eta'$ channel there is evidence for the $f_0(1500)$ and a peak at 1.95 GeV. The $\eta'\eta'$ channel shows a peak at threshold which is compatible with having $J^{PC} = 2^{++}$ and spin projection $J_Z = 0$.

Submitted to Physics Letters

1 LAPP-IN2P3, Annecy, France.
2 Athens University, Physics Department, Athens, Greece.
3 School of Physics and Astronomy, University of Birmingham, Birmingham, U.K.
4 CERN - European Organization for Nuclear Research, Geneva, Switzerland.
5 IHEP, Protvino, Russia.
6 IISN, Belgium.
7 JINR, Dubna, Russia.
8 High Energy Accelerator Research Organization (KEK), Tsukuba, Ibaraki 305-0801, Japan.
9 Faculty of Engineering, Miyazaki University, Miyazaki 889-2192, Japan.
10 RCNP, Osaka University, Ibaraki, Osaka 567-0047, Japan.
11 Oslo University, Oslo, Norway.
12 Faculty of Science, Tohoku University, Aoba-ku, Sendai 980-8577, Japan.

The $\eta\eta$, $\eta\eta'$ and $\eta'\eta'$ channels are considered to be promising places to look for glueballs since it is thought likely that glueballs will decay with the emission of ηs and η's [1]. Central production is proposed as a good place to search for glueballs via Double Pomeron Exchange (DPE) [2]. However, to date, only the $\eta\eta$ channel has been studied in this production mechanism [3]. In fact the $\eta'\eta'$ channel has only ever been observed once and that was by the VES experiment in the reaction $\pi^- p \to \eta'\eta' n$ where they observed 14 events [4].

In this paper a study is presented of the $\eta\eta'$ and $\eta'\eta'$ final states formed in the reaction

$$pp \to p_f(X^0)p_s \tag{1}$$

at 450 GeV/c. The data come from the WA102 experiment which has been performed using the CERN Omega Spectrometer, the layout of which is described in ref. [5].

Reaction (1), with X^0 being the $\eta\eta'$ final state has been isolated using the following decay modes:

$$\begin{array}{cc}
\eta \to \gamma\gamma & \eta' \to \eta\pi^+\pi^-, \eta \to \gamma\gamma \\
\eta \to \gamma\gamma & \eta' \to \eta\pi^+\pi^-, \eta \to \pi^+\pi^-\pi^0 \\
\eta \to \pi^+\pi^-\pi^0 & \eta' \to \eta\pi^+\pi^-, \eta \to \gamma\gamma \\
\eta \to \gamma\gamma & \eta' \to \rho^0(770)\gamma, \rho^0(770) \to \pi^+\pi^-
\end{array}$$

Other decay modes are possible but they have been found either to have too much combinatorial background or have too few events due to the small branching fraction of the η'. The above decay modes account for 26.5 % of the total. The $\rho^0(770)$ is observed decaying to $\pi^+\pi^-$ and is selected by requiring $0.7 \leq$ M($\pi^+\pi^-$) ≤ 0.84 GeV.

Fig. 1a) shows a scatter plot of $M(\gamma\gamma)$ against $M(\eta\pi^+\pi^-)$ with $\eta \to \gamma\gamma$ which has been extracted from the sample of events having two outgoing central charged tracks and four γs reconstructed in the GAMS-4000 calorimeter using momentum and energy balance. A clear signal of the $\eta\eta'$ channel can be observed. Fig. 1e) shows the $\gamma\gamma$ mass spectrum if the $\eta\pi^+\pi^-$ is compatible with being an η' ($0.9 \leq$ M($\eta\pi^+\pi^-$) ≤ 1.02 GeV) where a clear η signal can be observed. Fig. 1f) shows the $\eta\pi^+\pi^-$ mass spectrum if the $\gamma\gamma$ is compatible with being an η ($0.45 \leq$ M($\gamma\gamma$) ≤ 0.65 GeV) where a clear η' signal can be observed. The $\eta\eta'$ final state has been selected using the mass cuts described above.

Fig. 1b) shows a scatter plot of $M(\gamma\gamma)$ against M($\eta\pi^+\pi^-$) with $\eta \to \pi^+\pi^-\pi^0$ for the sample of events having four outgoing central charged tracks and four γs reconstructed in the GAMS-4000 calorimeter after imposing momentum and energy balance. A clear signal of the $\eta\eta'$ channel can be observed. The $\eta\eta'$ final state has been selected by requiring that the $0.45 \leq$ M($\gamma\gamma$) ≤ 0.65 GeV and $0.9 \leq$ M($\eta\pi^+\pi^-$) ≤ 1.02 GeV. Fig. 1c) shows a scatter plot of $M(\pi^+\pi^-\pi^0)$ against $M(\eta\pi^+\pi^-)$ with $\eta \to \gamma\gamma$ for the the sample of events having four outgoing central charged tracks and four γs reconstructed in the GAMS-4000 calorimeter after imposing momentum and energy balance. A signal of the $\eta\eta'$ channel can be observed. The $\eta\eta'$ final state has been selected by requiring that the $0.5 \leq$ M($\pi^+\pi^-\pi^0$) ≤ 0.6 GeV and $0.9 \leq$ M($\eta\pi^+\pi^-$) ≤ 1.02 GeV. Fig. 1d) shows a scatter plot of $M(\gamma\gamma)$ against $M(\rho^0(770)\gamma)$ for the the sample of events having two outgoing central charged tracks and three γs reconstructed in the GAMS-4000 calorimeter after imposing momentum and energy balance. A signal of the $\eta\eta'$ channel can be observed. The $\eta\eta'$ final state has been selected by requiring that the $0.45 \leq$ M($\gamma\gamma$) ≤ 0.65 GeV and $0.9 \leq$ M($\rho^0(770)\gamma$) ≤ 1.02 GeV.

The background varies from 30 % to 50 % dependent on the decay topology. The total background in the combined $\eta\eta'$ mass spectrum is 38 % of the data. In order to determine the effect of this background events that have the same final state particles but do not balance momentum have been studied. There is no signal for the η or η' in the corresponding mass spectra but the distributions do represent the background in the data quite well. The effect of this background in the $\eta\eta'$ mass spectrum is a smooth distribution that reaches a maximum at 1.8 GeV.

The resulting $\eta\eta'$ mass spectra from each channel are very similar and the combined mass spectrum is shown in fig. 2a) and consists of 872 events. The mass spectrum has a threshold enhancement and a shoulder around 1.95 GeV. In previous analyses of the $\eta\eta'$ system by Crystal Barrel [6] and NA12 [7] this threshold has been interpreted as being due to the $f_0(1500)$.

In order to determine the spin of the $\eta\eta'$ system, an analysis has been performed assuming that the $\eta\eta'$ system is produced by the collision of two particles (referred to as exchanged particles) emitted by the scattered protons. The z axis is defined by the momentum vector of the exchanged particle with the greatest four-momentum transferred in the $\eta\eta'$ centre of mass. The y axis is defined by the cross product of the two exchanged particles momenta in the pp centre of mass. The two variables needed to specify the decay process were taken as the polar and azimuthal angles (θ, ϕ) of the η in the $\eta\eta'$ centre of mass relative to the coordinate system described above.

Fig. 2c) shows the acceptance corrected $\cos(\theta)$ distribution for the $f_0(1500)$ region. The distribution is flat as would be expected for a spin 0 particle. A fit has been performed to the mass spectrum using a Flatté like formula [8] to describe the $f_0(1500)$, a Breit-Wigner to describe the shoulder at 1.95 GeV and a background of the form $a(m - m_{th})^b exp(-cm - dm^2)$, where m is the $\eta\eta'$ mass, m_{th} is the $\eta\eta'$ threshold mass and a, b, c, d are fit parameters. The resulting fit is shown in fig. 2a) and gives sheet II pole positions [9] for the $f_0(1500)$ of

$$f_0(1500) \qquad \mathrm{M} = (1515 \pm 12) \quad -i\,(\;55 \pm 12) \qquad \mathrm{MeV}$$

These parameters are consistent with the PDG [10] values for the $f_0(1500)$. For the peak at 1.95 GeV the fit gives

$$\mathrm{M} \;=\; 1934 \pm\; 16 \quad \mathrm{MeV}, \qquad \Gamma \;=\; 141 \;\pm\; 41 \quad \mathrm{MeV}$$

These parameters are similar to those found in the $\eta\eta'$ final state by the NA12 experiment [11] which they claimed may have an exotic nature. The PDG [10] have listed this observation with a state seen with similar mass and width in the $\omega\omega$ final state which has been found to have $J^{PC} = 2^{++}$. This state is called the $X(1910)$ by the PDG [10]. The background distribution found from the fit is similar in size and shape to that which was determined by using events that do not balance momentum described above.

In order to try to learn more about the spin of the peak at 1.95 GeV, the $\eta\eta'$ mass spectrum has been fitted in four intervals of $\cos(\theta)$ and the number of events in each bin determined from the fit. The resulting $\cos(\theta)$ distribution is shown in fig. 2d). Superimposed on the distribution are the three spin hypotheses which best describe the data. The solid curve represents a $J^{PC} = 0^{++}$ state, the dashed curve a $J^{PC} = 1^{-+}$ with spin projection $|J_Z|$ =1 and the dotted curve a $J^{PC} = 2^{++}$ with spin projection $|J_Z|$ =2. All other spin projections can be discounted. It should be noted that no evidence has previously been found in central production for a resonance with spin projection $|J_Z| = 2$. Further information will come from an analysis of the centrally produced $\omega\omega$ system which is in progress.

It is possible to decrease the χ^2/NDF of the fit to the mass spectrum from 16/15 to 10/12 by introducing a third Breit-Wigner in the 2.4 GeV region. The resulting parameters for this Breit-Wigner are M = 2369 $\pm$ 10 MeV, Γ = 52 $\pm$ 31 MeV. If this were interpreted as a resonance it could be due to the $f_2(2340)$ which has been observed in the centrally produced $\phi\phi$ final state [12].

In previous analyses a study has been made of how different resonances are produced as a function of the parameter dP_T, which is the difference in the transverse momentum vectors of the two exchange particles [5], and of the azimuthal angle ϕ which is defined as the angle between the p_T vectors of the two outgoing protons.

In order to learn more about the resonances produced in the $\eta\eta'$ channel a study has been made of the dP_T and ϕ dependences. These dependences are consistent with the threshold region being due to the $f_0(1500)$ [13].

Correcting for the unseen decay modes and the effects of the detector the branching ratio of the $f_0(1500)$ to $\eta\eta'$ $/\pi\pi$ is determined to be 0.095 $\pm$ 0.026, consistent with the value that is derived from the PDG [10] of 0.066 $\pm$ 0.033.

After taking into account the background, correcting for geometrical acceptances, detector efficiencies, losses due to cuts and unseen decay modes, the cross-section for the $\eta\eta'$ channel at $\sqrt{s}$ = 29.1 GeV in the x_F interval $|x_F| \leq 0.2$ is $\sigma(\eta\eta'\ )$ = 145 $\pm$ 18 nb. Above the $\eta'\eta'$ threshold the cross section is 53 $\pm$ 10 nb.

The remainder of this paper describes the $\eta'\eta'$ channel. Reaction (1), with X^0 being the $\eta'\eta'$ final state has been isolated using the following decay modes:

$$\begin{array}{rr}
\eta' \to \rho^0(770)\gamma & \eta' \to \rho^0(770)\gamma \\
\eta' \to \rho^0(770)\gamma & \eta' \to \eta\pi^+\pi^-, \eta \to \gamma\gamma \\
\eta' \to \eta\pi^+\pi^-, \eta \to \gamma\gamma & \eta' \to \eta\pi^+\pi^-, \eta \to \gamma\gamma
\end{array}$$

Other decay modes are possible but they have been found either to have too much combinatorial background or have too few events due to the small branching fraction of the η'. The above decay modes account for 22.4 % of the total.

Fig. 3a) shows a scatter plot of $M(\rho^0(770)\gamma)$ against $M(\rho^0(770)\gamma)$ which has been extracted from the sample of events having four outgoing central charged tracks and two γs reconstructed in the GAMS-4000 calorimeter using momentum and energy balance. A clear signal of the $\eta'\eta'$ channel can be observed. Fig. 3b) shows the $\rho^0(770)\gamma$ mass spectrum if the other $\rho^0(770)\gamma$ mass is compatible with being an η' ($0.9 \leq M(\rho^0(770)\gamma) \leq 1.02$ GeV) where a clear η' signal can be observed. The $\eta'\eta'$ final state has been selected using the mass cuts described above.

Fig. 3c) shows a scatter plot of $M(\rho^0(770)\gamma)$ against $M(\eta\pi^+\pi^-)$ with the η decaying to $\gamma\gamma$ which has been extracted from the sample of events having four outgoing central charged tracks and three γs reconstructed in the GAMS-4000 calorimeter using momentum and energy balance. A clear signal of the $\eta'\eta'$ channel can be observed. Fig. 3d) shows the $\rho^0(770)\gamma$ mass spectrum if the $\eta\pi^+\pi^-$ mass is compatible with being an η' ($0.9 \leq$ M($\eta\pi^+\pi^-$) ≤ 1.02 GeV) and fig 3e) shows the $\eta\pi^+\pi^-$ mass spectrum if the $\rho^0(770)\gamma$ mass is compatible with being an η'. In both cases a clear η' signal can be observed. The $\eta'\eta'$ final state has been selected using the mass cuts described above.

Fig. 3f) shows a scatter plot of $M(\eta\pi^+\pi^-)$ against $M(\eta\pi^+\pi^-)$ with both ηs decaying to $\gamma\gamma$ which has been extracted from the sample of events having four outgoing central charged tracks and four γs reconstructed in the GAMS-4000 calorimeter using momentum and energy balance. A clear signal of the $\eta'\eta'$ channel can be observed. Fig. 3g) shows the $\eta\pi^+\pi^-$ mass spectrum if the other $\eta\pi^+\pi^-$ mass is compatible with being an η' ($0.9 \leq$ M($\eta\pi^+\pi^-$) ≤ 1.02 GeV) where a clear η' signal can be observed. The $\eta'\eta'$ final state has been selected using the mass cuts described above.

The background varies from 23 % to 55 % dependent on the decay topology. The total background in the combined $\eta\eta'$ mass spectrum is 36 % of the data. In order to determine the effect of this background events that have the same final state particles but do not balance momentum have been studied. There is no signal for the η' in the corresponding mass spectra but the distributions do represent the background in the data quite well. The effect of this background in the $\eta'\eta'$ mass spectrum is a smooth distribution that reaches a maximum at 2.2 GeV.

The resulting $\eta'\eta'$ mass spectra from each channel are very similar and the combined mass spectrum consists of 166 events and is shown in fig. 4a) in 40 MeV bins and in fig. 4b) in 80 MeV bins. The mass spectrum has a peak around 2 GeV.

Fig. 4c) shows the acceptance corrected $\cos(\theta)$ distribution for the 2 GeV region. The distribution is not flat. Superimposed on the distribution is the result of a fit to the distribution of the form $\alpha + \beta(3/2cos^2\theta - 1/2)^2$ representing what would be expected for a spin 2 particle with spin projection $J_Z = 0$ and a flat background. The fit well reproduces the data and gives $\alpha = 1.5$ and $\beta = 9.0$.

A fit has been performed to the mass spectrum using a Breit-Wigner to describe the 2 GeV region and a background of the form $a(m - m_{th})^b exp(-cm - dm^2)$, where m is the $\eta'\eta'$ mass, m_{th} is the $\eta'\eta'$ threshold mass and a, b, c, d are fit parameters. The fit results in $M = 2007 \pm 24$ MeV, $\Gamma = 90 \pm 43$ MeV. Based on the mass and width of this state and taking into account the $\eta'\eta'$ threshold this peak could be described as being due to the $X(1910)$ observed in the $\eta\eta'$ channel. However the spin projection found for the $X(1910)$ is completely different.

The broad distribution, described as the background above, is compatible in shape with what would be expected from the $f_2(1950)$ observed decaying to $f_2(1270)\pi\pi$ which also has possible $\phi\phi$ and $K^*\overline{K}^*$ decay modes [12]. In order to see if the $f_2(1950)$ does have an $\eta'\eta'$ decay mode a study has been made of the dP_T and ϕ dependences of the $\eta'\eta'$ channel. The fraction of $\eta'\eta'$ events has been calculated for $dP_T\leq0.2$ GeV, $0.2\leq dP_T\leq0.5$ GeV and $dP_T\geq0.5$ GeV and gives 0.10 ± 0.03, 0.44 ± 0.05 and 0.46 ± 0.05 respectively. This results in a ratio of production at small dP_T to large dP_T of 0.22 ± 0.07. The azimuthal angle (ϕ) between the p_T vectors of the two protons is shown in fig. 4d). Both the dP_T and ϕ distributions are different to what was observed for the $f_2(1950)$ [12] and hence would suggest that the $\eta'\eta'$ channel is not mainly due to the $f_2(1950)$.

After taking into account the background, correcting for geometrical acceptances, detector efficiencies, losses due to cuts, and unseen decay modes, the cross-section for the $\eta'\eta'$ channel at $\sqrt{s}$ = 29.1 GeV in the x_F interval $|x_F| \leq 0.2$ is $\sigma(\eta'\eta'\ ) = 146 \pm 24$ nb.

In summary, a study of the $\eta\eta'$ and $\eta'\eta'$ channels has been performed for the first time in central production. The $\eta'\eta'$ channel has been observed with more than a factor of 10 times the statistics of the only other previous observation of this channel in any production mechanism [4]. In the $\eta\eta'$ channel there is evidence for the $f_0(1500)$ and a peak at 1.95 GeV. The $\eta'\eta'$ channel shows a peak at threshold which is compatible with having $J^{PC} = 2^{++}$ and spin projection $J_Z = 0$.

Acknowledgements

This work is supported, in part, by grants from the British Particle Physics and Astronomy Research Council, the British Royal Society, the Ministry of Education, Science, Sports and Culture of Japan (grants no. 07044098 and 1004100), the French Programme International de Cooperation Scientifique (grant no. 576) and the Russian Foundation for Basic Research (grants 96-15-96633 and 98-02-22032).

References

[1] S. S. Gershtein *et al.,* Zeit. Phys. **C24** (1984) 305;
R. Akhoury and J.M. Frere, Phys. Lett. **B220** (1989) 258.

[2] D. Robson *et al.,* Nucl. Phys. **B130** (1977) 328;
F. E. Close, Rep. Prog. Phys. **51** (1988) 833.

[3] D. Alde *et al.,* Phys. Lett. **B201** (1988) 160;
A. Singovski, Il Nouvo Cimento **A107** (1993) 1911.

[4] G. M. Beladidze *et al.,* Zeit. Phys. **C57** (1992) 13.

[5] D. Barberis *et al.,* Phys. Lett. **B397** (1997) 339.

[6] C. Amlser *et al.,* Phys. Lett. **B353** (1995) 571.

[7] F. Binon *et al.,* Il Nouvo Cimento **A80** (1994) 363.

[8] S.M. Flatté, Phys. Lett. **B38** (1972) 232.

[9] D. Morgan, Phys. Lett. **B51** (1974) 71.

[10] Particle Data Group, European Physical Journal **C3** (1998) 1.

[11] D. Alde *et al.,* Phys. Lett. **B216** (1989) 447.

[12] D. Barberis *et al.,* In preparation.

[13] D. Barberis *et al.,* Phys. Lett. **B462** (1999) 462.

Figures

Figure 1: Selection of the $\eta\eta'$ final state. a) $M(\gamma\gamma)$ versus $M(\eta\pi^+\pi^-)$ with $\eta \to \gamma\gamma$, b) $M(\gamma\gamma)$ versus M($\eta\pi^+\pi^-$) with $\eta \to \pi^+\pi^-\pi^0$, c) $M(\pi^+\pi^-\pi^0)$ versus $M(\eta\pi^+\pi^-)$ with $\eta \to \gamma\gamma$, d) $M(\gamma\gamma)$ versus $M(\eta\pi^+\pi^-)$ with $\eta \to \rho^0(770)\gamma$, e) M($\gamma\gamma$) if ($0.9 \leq$ M($\eta\pi^+\pi^-$) ≤ 1.02 GeV) and f) shows the M($\eta\pi^+\pi^-$) if ($0.45 \leq$ M($\gamma\gamma$) ≤ 0.65 GeV).

Figure 2: a) and b) the $\eta\eta'$ mass spectrum with fit described in the text. The $\cos(\theta)$ distribution a) for the $f_0(1500)$ region and b) for the 1.95 GeV region.

Figure 3: Selection of the $\eta'\eta'$ final state. a) M($\rho^0(770)\gamma$) versus M($\rho^0(770)\gamma$), b) the M($\rho^0(770)\gamma$) distribution if the other M($\rho^0(770)\gamma$) distribution is compatible with being an η'. c) M($\eta\pi^+\pi^-$) versus M($\rho^0(770)\gamma$), d) the M($\rho^0(770)\gamma$) distribution if M($\eta\pi^+\pi^-$) distribution is compatible with being an η'. e) the M($\eta\pi^+\pi^-$) distribution if M($\rho^0(770)\gamma$) distribution is compatible with being an η'. f) M($\eta\pi^+\pi^-$) versus M($\eta\pi^+\pi^-$) and g) the M($\eta\pi^+\pi^-$) distribution if the other M($\eta\pi^+\pi^-$) is compatible with being an η'.

Figure 4: a) and b) the $\eta'\eta'$ mass distribution with fit described in the text. c) The $\cos(\theta)$ distribution for the $1.9 - 2.1$ GeV region. d) the ϕ distribution for the $\eta'\eta'$ channel.

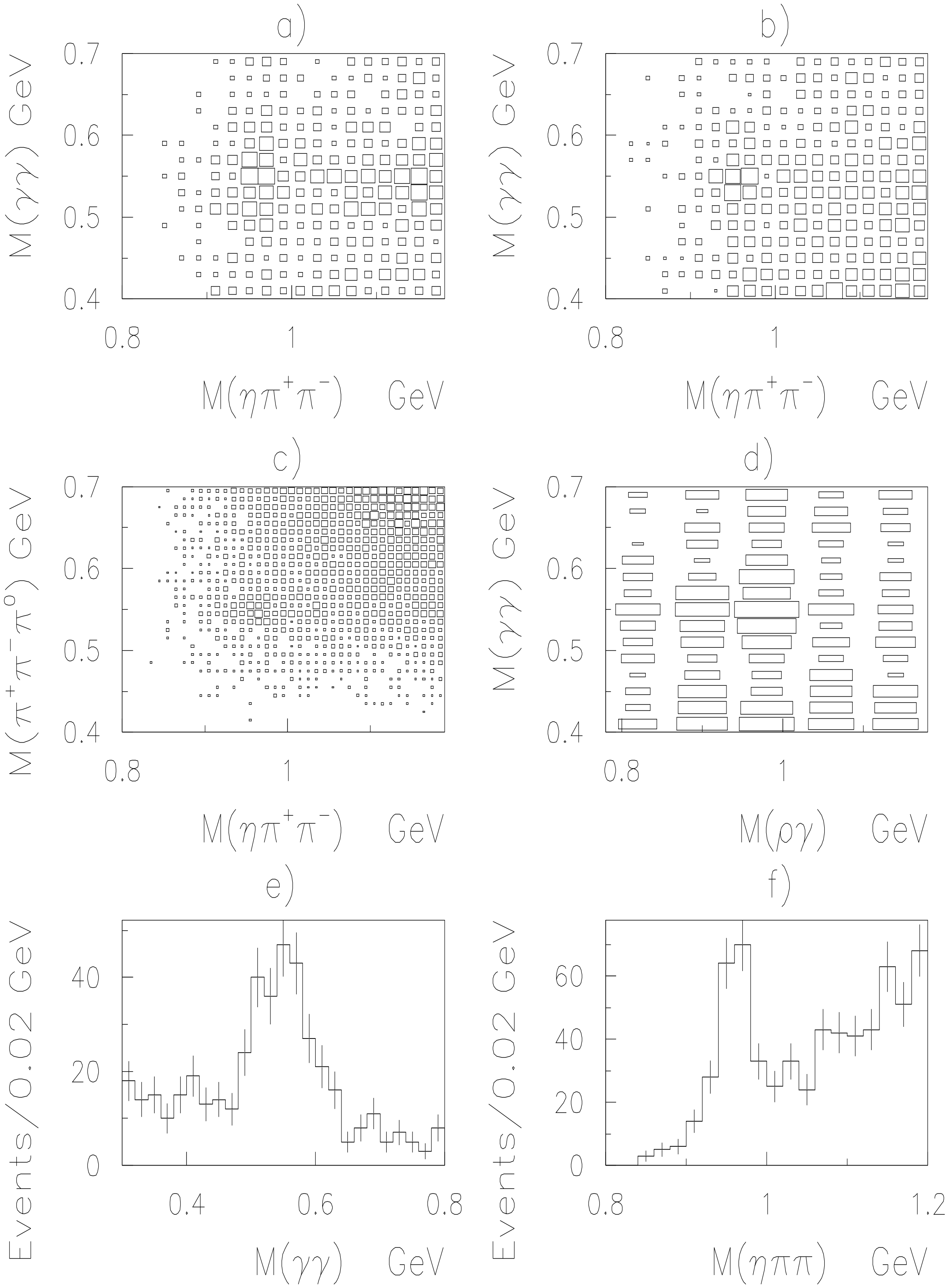
a)
M(γγ) GeV
M(ηπ⁺π⁻) GeV
b)
M(γγ) GeV
M(ηπ⁺π⁻) GeV
c)
M(π⁺π⁻π⁰) GeV
M(ηπ⁺π⁻) GeV
d)
M(γγ) GeV
M(ργ) GeV
e)
Events/0.02 GeV
M(γγ) GeV
f)
Events/0.02 GeV
M(ηππ) GeV

Figure 1

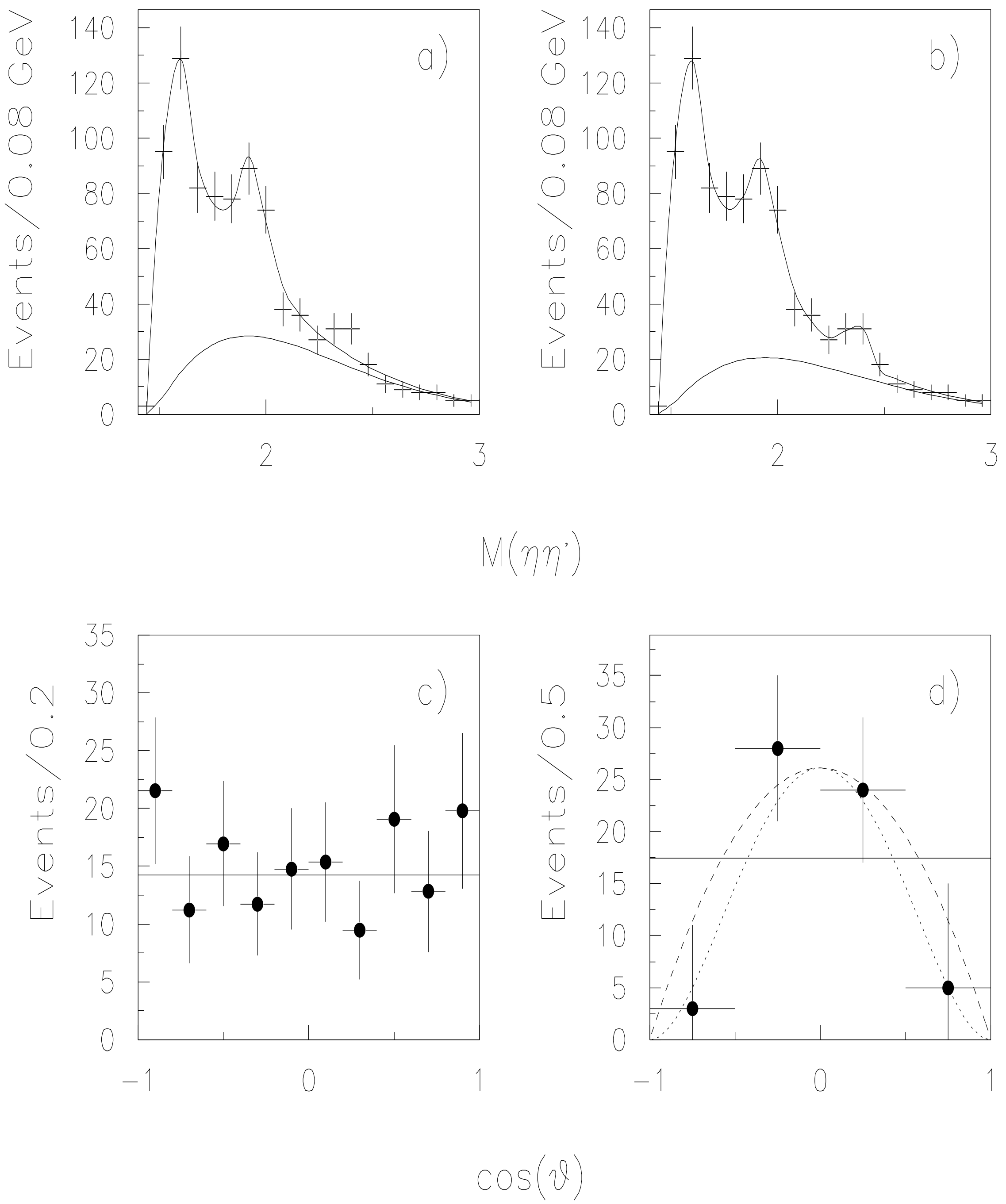

Figure 2

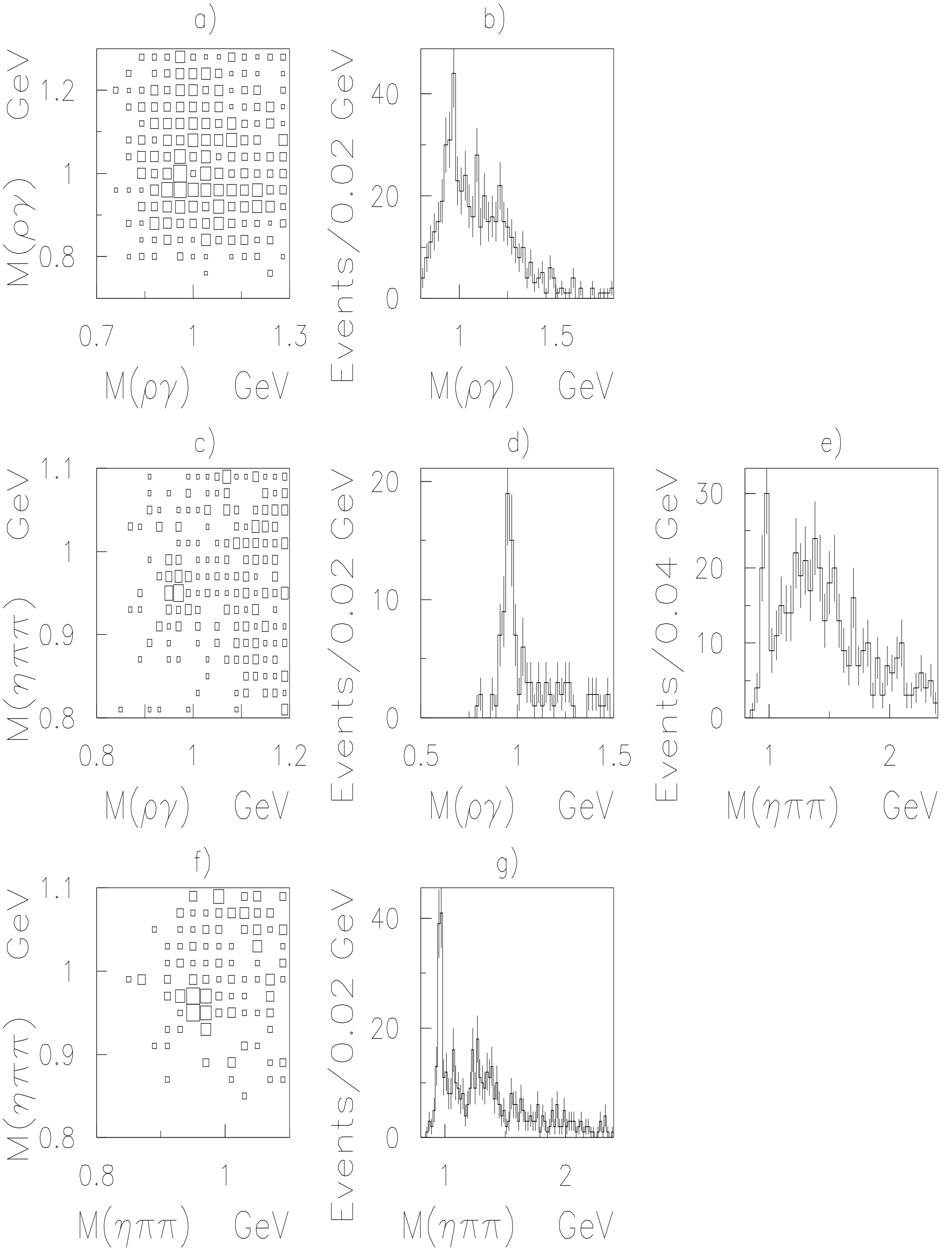

Figure 3

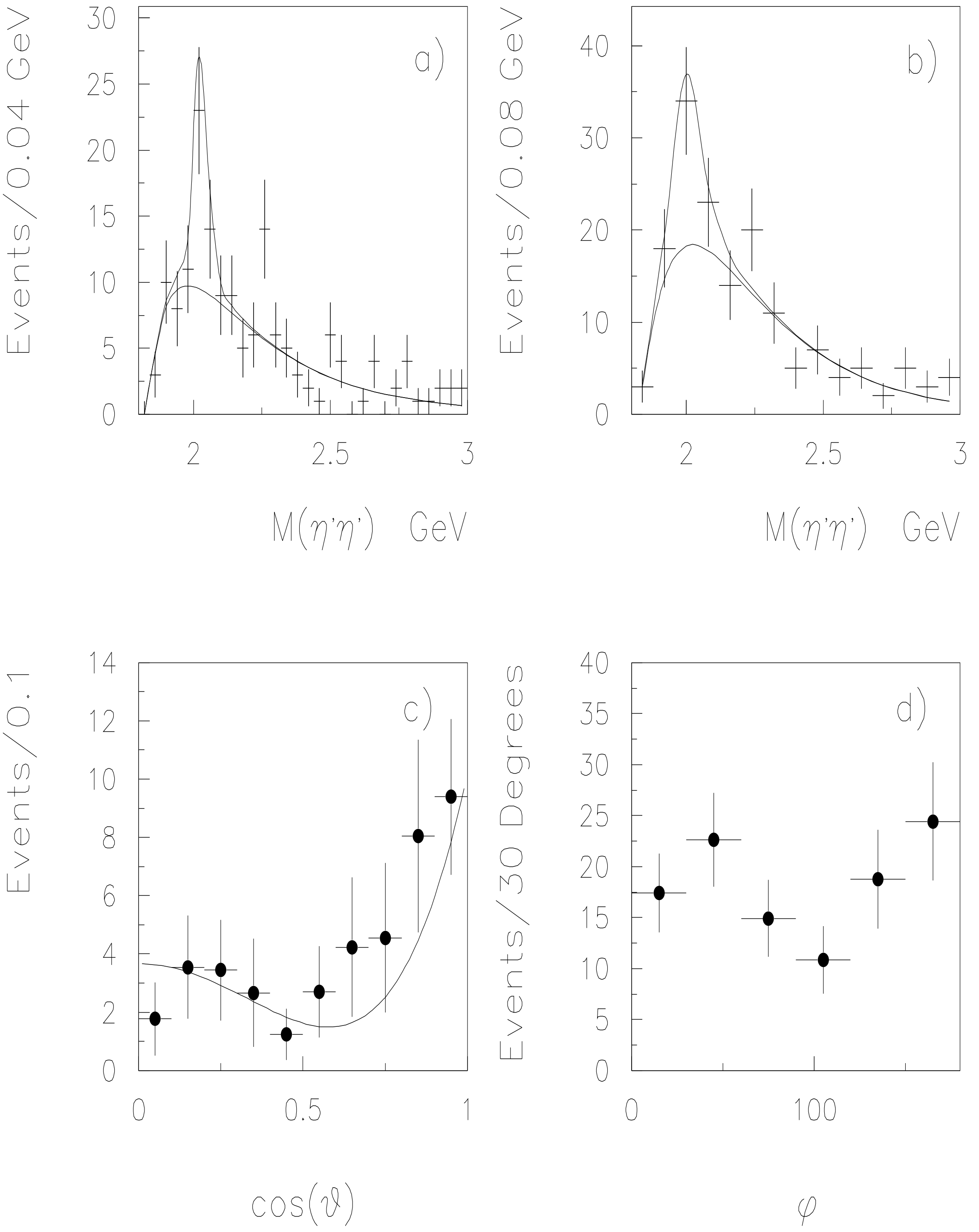

Events/0.04 GeV
a)
M(η'η') GeV
Events/0.08 GeV
b)
M(η'η') GeV
Events/0.1
c)
cos(ϑ)
Events/30 Degrees
d)
φ

Figure 4